with Eq. (11), we get the Hayes' formulas for the vorticity jump, which are

$$\delta(\zeta_n) = 0 \tag{12c}$$

$$\delta\zeta_t = \boldsymbol{n} \times \left\{ \delta\left(\frac{1}{\rho}\right) \frac{\partial}{\partial x^\alpha}(\rho q_r)\boldsymbol{a}^\alpha - \frac{\delta(\rho)}{\rho q_r} \times \left[\frac{\partial \boldsymbol{q}_t}{\partial \tau} + \frac{\partial \boldsymbol{q}_t}{\partial x^\alpha}\boldsymbol{a}^\alpha \cdot \boldsymbol{v}_t - q_s \frac{\partial q_s}{\partial x^\alpha}\boldsymbol{a}^\alpha - (\boldsymbol{R} \cdot q_t) q_s \right] \right\} \tag{12d}$$

As should be expected, Eq. (12d) can be reduced to Eq. (30) of Ref. 1 when $\partial/\partial\tau$ is expressed in terms of $\partial/\partial t$ through Eq. (5b). Note that only the surface tangential part of the derivatives of $\boldsymbol{q}_t$ have to be retained in Eq. (12d). As has been noted by Hayes[1] and also by Isom and Kalkhoran,[2] the importance of Eq. (12d) lies in the fact that it is independent of any thermodynamic law.

As has been noted earlier, the surface curvature tensor $\boldsymbol{R}$ given in Eqs. (7) is symmetric. If, however, one uses the representation (7b), then the matrix formed by the mixed components is a nonsymmetric matrix, i.e.,

$$\boldsymbol{R} = \begin{bmatrix} b_{1\beta} g^{\beta 1} & b_{2\beta} g^{\beta 1} \\ b_{1\beta} g^{\beta 2} & b_{2\beta} g^{\beta 2} \end{bmatrix}$$

The use of the preceding matrix directly yields the sum of the principal curvature and the Gaussian curvature of the shock surface, i.e.,

$$\begin{aligned} \mathrm{tr}(\boldsymbol{R}) &= k_I + k_{II}, \qquad \text{sum of the principal curvatures} \\ \det(\boldsymbol{R}) &= K, \qquad \text{Gaussian curvature} \end{aligned} \tag{13}$$

From Warsi,[7] the physical components of $\boldsymbol{R}$ are

$$R(\beta\delta) = (g_{\beta\beta}/g_{\delta\delta})^{\frac{1}{2}} R_{\alpha\delta} g^{\alpha\beta} \tag{14}$$

(sum on α, and $R_{\alpha\delta} = b_{\alpha\delta}$). The matrix formed by the components given in Eq. (14) is again a nonsymmetric matrix, and its trace and determinant are the same as stated in Eq. (13). The terms appearing in Eqs. (13) and (14) can directly be computed by the coordinate generation program.

Conclusion

Hayes' vorticity jump conditions have been obtained in general shock surface oriented coordinates. The main formula (12d) exhibits Hayes' tangential vorticity jump formula in time and space coordinates attached to the shock surface. It can be incorporated in a flow code that uses moving and deforming coordinates attached to a shock. Because the coordinates are time dependent, they have to be regenerated at every time step. Note that $\boldsymbol{R}$ is a function of time because the coefficients of the first and the second fundamental forms ($g_{\alpha\beta}$, $b_{\alpha\beta}$) are functions of time.

References

[1]Hayes, W. D., "The Vorticity Jump Across a Gasdynamic Discontinuity," *Journal of Fluid Mechanics*, Vol. 2, Aug. 1957, pp. 595–600.

[2]Isom, M. P., and Kalkhoran, I. M., "Comment on the Vorticity Jump Across a Shock Wave," *AIAA Journal,* Vol. 34, No. 12, 1996, p. 2640.

[3]Emanuel, G., "Reply to M. P. Isom and I. M. Kalkhoran," *AIAA Journal,* Vol. 34, No. 12, 1996, p. 2641.

[4]Warsi, Z. U. A., "Numerical Grid Generation in Arbitrary Surfaces Through a Second-Order Differential Geometric Model," *Journal of Computational Physics,* Vol. 64, No. 1, 1986, pp. 82–96.

[5]Warsi, Z. U. A., *Fluid Dynamics: Theoretical and Computational Approaches*, CRC Press, Boca Raton, FL, 1993.

[6]Warsi, Z. U. A., "Theoretical Foundation of the Equations for the Generation of Surface Coordinates," *AIAA Journal,* Vol. 28, No. 6, 1990, pp. 1140–1142.

[7]Warsi, Z. U. A., "Operations on the Physical Components of Tensors," ZAMM, Vol. 76, No. 6, 1996, pp. 361–363.

W. Oberkampf
Associate Editor

Generalized Vortex Lattice Method for Planar Supersonic Flow

Paulo A. O. Soviero*
Instituto Tecnológico de Aeronáutica, São José dos Campos, Brazil
and
Hugo B. Resende†
Empresa Brasileira de Aeronáutica S.A., São José dos Campos, Brazil

Introduction

THE problem of a lifting surface oscillating harmonically in supersonic flow has been studied by several researchers of unsteady aerodynamics. However, if one considers classical linearized models, there is a wide number of available numerical methods of solution, implying that there is not a preferred, well-accepted way to solve for the pressure distribution over thin wings for a known movement. The reader is referred to Yates[1] for a complete review and discussion of the state of the art of unsteady aerodynamics. According to that work, the analysis problem of supersonic lifting surfaces may be classified into four numerical models. In the first one, called the integrated-pressure method, the acceleration potential is used as the main variable, and it is related to the downwash over the wing by means of an integral equation.[2–5] This model comes directly from the subsonic case and has similar methods of solution. The second model is based on the superposition of velocity potential sources over the wing, with the magnitudes given by an integral of the downwash, usually obtained numerically.[6,7] In this formulation, the upper and lower surfaces of the wing must be isolated from each other; that is, from a physical point of view, all the edges of the wing must be supersonic. If any edge is subsonic, there is a region where the lower and upper surfaces interact, and diaphragms must be employed. In the third and fourth models, called integrated-potential[8] and potential-gradient[9,10] methods, respectively, the velocity potential is used as the main variable and the integral equation relates the downwash to the velocity potential difference between the upper and lower surfaces of the wing and wake. Because the kernel function is related to a velocity potential source, and double differentiation normal to the planform is performed after integration, the main difference between those numerical methods comes from the way the kernel function is manipulated prior to integration. Finally, although the velocity potential formulations just reviewed are widespread, they are not immediately evident to the aerodynamicist because their well-known singular solutions as sources, doublets, and line vortices are hardly identifiable after so many integrations by parts, new variable definitions, or series expansions.

The present work considers the velocity potential formulation of supersonic, harmonically oscillating lifting surfaces. The problem is linearized and, therefore, limited to small disturbances and flat wakes, with the solution being obtained numerically. Both the wing and the wake are discretized by means of constant density doublet panels, and the complex potential results are obtained through the solution of the hyperbolic Helmholtz equation.[11] The equivalence between closed vortex loops and surfaces of constant density potential remains valid in the steady-state case,[12] leading to the not-so-widespread supersonic version[13] of the well-known incompressible vortex lattice method. Therefore, in the present work the generalized vortex lattice method for oscillating lifting surfaces in

Received April 22, 1996; presented as Paper 96-2491 at the AIAA 14th Applied Aerodynamics Conference, New Orleans, LA, June 17–20, 1996; revision received March 7, 1997; accepted for publication March 11, 1997.

*Professor, Aeronautical Engineering Division. Member AIAA.
†Aeroelastic Engineer, Structure Department. Member AIAA.

subsonic flow[14] is extended to the supersonic planar regime; that is, the method of solution for the subsonic and supersonic regimes is unified. Also, the present formulation can be classified as an integrated-downwash method, where the source solution is substituted by a doublet one.

Mathematical Flow Model and Integral Equation

In a reference frame that translates uniformly with the undisturbed flow velocity U, the perturbation velocity potential due to the small-amplitude motion of a thin wing is governed by the linear convected wave equation. After transformations,[11,15] one obtains the hyperbolic Helmholtz equation

$$\frac{\partial^2\Phi}{\partial x^2} - \frac{\partial^2\Phi}{\partial y^2} - \frac{\partial^2\Phi}{\partial z^2} + K^2\Phi = 0 \tag{1}$$

Note that Φ is the perturbation velocity potential, whereas the term in K^2 determines how much the reduced potential equation departs from the canonical wave equation, which governs steady supersonic flow. The reduced frequency is defined here as $k_r = \omega c/2U$, whereas $K = k_r M/\beta^2$, where ω is the angular frequency of the motion, M is the Mach number of the undisturbed flow, and $\beta^2 = M^2 - 1$.

The small-disturbance boundary condition on the wing surface may be written as

$$\frac{\partial\Phi}{\partial z} = w(x, y) = \frac{\exp(iKMx)}{\beta}\left[\frac{\partial h}{\partial x} + ik_r h\right] \tag{2}$$

where $h(x, y)$ represents the wing vertical displacement. The complex pressure coefficient is given by

$$C_p = -2\exp(-iKMx)\left[\frac{\partial\Phi}{\partial x} - i\frac{K}{M}\Phi\right] \tag{3}$$

When this expression is applied to both sides of the wake, pressure continuity is ensured if

$$\delta C_p = 0 = \frac{\partial\delta\Phi}{\partial x} - i\frac{K}{M}\delta\Phi \tag{4}$$

Note that $\delta\Phi$ and δC_p indicate the velocity potential and pressure coefficient jumps, respectively, between the lower and upper surfaces of the wake.

The solution of the problem just described is obtained from the integral equation that relates the potential jump across the lifting surface (and wake) to the downwash. For planar configurations

$$w(x, y) = -\frac{1}{2\pi}\int\!\!\int \delta\Phi\left[\frac{\cos Kr}{r^3} + \frac{K\sin Kr}{r^2}\right] \mathrm{d}x_0\,\mathrm{d}y_0 \tag{5}$$

The term between the brackets corresponds to the doublet induced normal velocity in the wing plane ($z = 0$), whereas $r = [(x - x_0)^2 - (y - y_0)^2]^{1/2}$ is the hyperbolic distance from the doublet placed at (x_0, y_0) to the receiving point (x, y). The integral sign must be taken in its usual way, that is, in the sense of the finite part integration over the appropriate area of influence. It can be stated from Eq. (5) that the integrand represents a normal doublet density $\delta\Phi$ distributed over an area element dS. When $\delta\Phi$ is assumed constant over each element, the integral equation may be written as

$$w(x, y) = -\frac{1}{2}\frac{\partial\delta\Phi}{\partial x}(x, y) - \frac{1}{2\pi}\int \mathrm{d}x_0 \int \delta\Phi\left[\frac{\cos Kr}{r^3} + \frac{K\sin Kr}{r^2}\right]\mathrm{d}y_0 \tag{6}$$

where only the integral along y_0 must be evaluated using the finite part concept. For each point (x, y) the domain of integration is defined by the Mach forecone emanating from it.

Numerical Solution

Solutions of the problem are obtained by solving integral equation (6) for $\delta\Phi$, using the boundary conditions (2) and (4) for the wing and wake surfaces, respectively. Both surfaces are discretized in small quadrilaterals of unknown constant density doublets. The boundary conditions are enforced at control points located at each panel geometrical center, which is equivalent to the usual $\frac{1}{4}$–$\frac{3}{4}$ rule. Finally, the numerical scheme that results from the discretization of

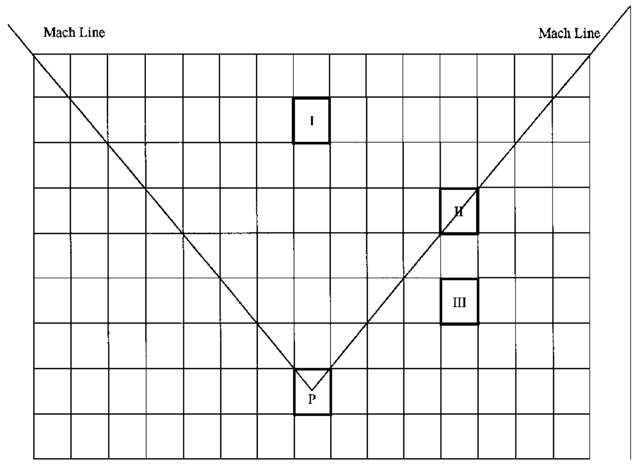

Fig. 1 Wing discretization: kinds of integration domains for receiving point.

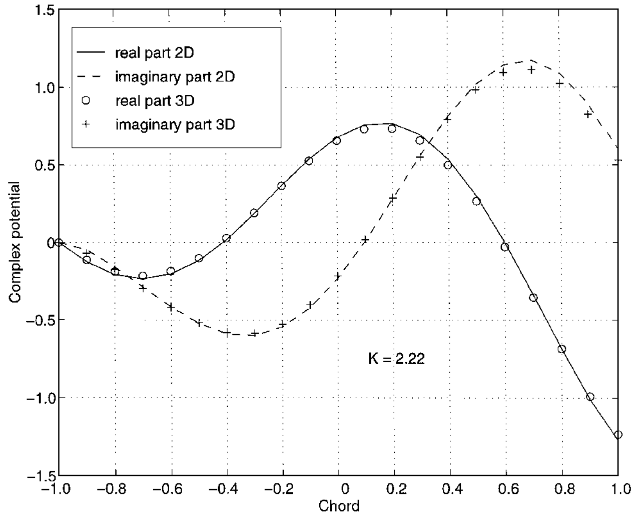

Complex velocity potential

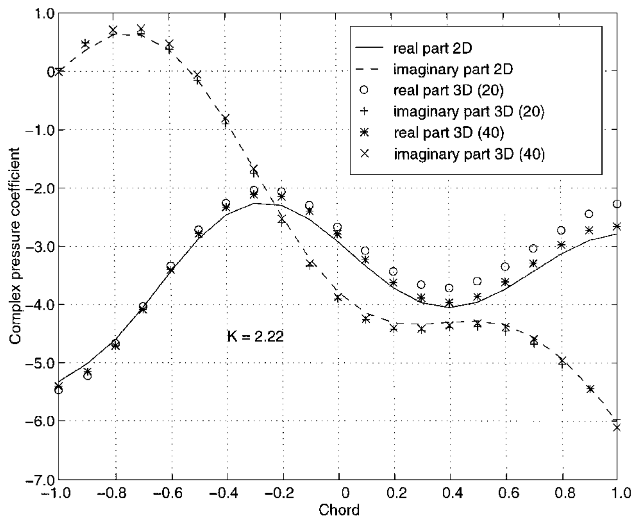

Complex pressure coefficient

Fig. 2 Unsteady results for wing pitching about the leading-edge axis: K = 2.22.

the equations corresponds to a system of linear equations, where the influence coefficient matrix is made of real elements.

The key features of the proposed method of solution are summarized in Fig. 1. One can identify three kinds of integration domain: I, completely inside the influence Mach cone; II, only partially inside the Mach cone; and III, completely outside the Mach cone, corresponding to zero influence. In region I the numerical integration is straightforward because r is never equal to zero, whereas in region II

Table 1 AGARD rectangular wing: aspect ratio equal to 2.0 and $c = 1.0$; mode: 1, heaving (amplitude 1.0) and 2, pitching about midchord (amplitude $\pi/4$)

			$k_r = 0$		$k_r = 0.15$		$k_r = 0.30$	
Method	Mach	Q_{mn}	Real	Imaginary	Real	Imaginary	Real	Imaginary
Present[a]	1.2	Q_{11}	——	——	0.187	1.011	0.342	1.642
Ref. 7[b]			——	——	0.189	1.000	0.348	1.620
Ref. 8			——	——	0.220	0.980	0.414	1.560
Ref. 9			——	——	0.215	1.070	0.472	1.715
Ref. 16[b]			——	——	0.205	1.060	0.749	1.820
Present[a]	1.2	Q_{12}	3.756	——	3.376	−0.493	2.848	−0.275
Ref. 7[b]			3.750	——	3.370	−0.500	2.840	−0.288
Ref. 8			3.800	——	3.340	−0.590	2.780	−0.386
Ref. 9			3.978	——	3.567	−0.593	2.938	−0.556
Ref. 16[b]			3.951	——	3.531	−0.545	3.058	−0.940
Present[a]	1.2	Q_{21}	——	——	−0.003	−0.135	−0.111	−0.293
Ref. 7[b]			——	——	−0.005	−0.141	−0.107	−0.285
Ref. 8			——	——	−0.008	−0.122	−0.114	−0.228
Ref. 9			——	——	−0.001	−0.132	−0.096	−0.300
Ref. 16[b]			——	——	−0.005	−0.141	−0.026	−0.310
Present[a]	1.2	Q_{22}	−0.378	——	−0.420	−0.163	−0.397	0.450
Ref. 7[b]			−0.368	——	−0.411	−0.165	−0.380	0.450
Ref. 8			−0.310	——	−0.350	−0.159	−0.280	0.414
Ref. 9			−0.370	——	−0.419	−0.157	−0.403	0.440
Ref. 16[b]			−0.398	——	−0.446	−0.177	−0.427	0.350
Present[a]	1.05	Q_{11}	——	——	0.015	1.095	0.099	2.018
Ref. 7[b]			——	——	0.019	1.088	0.124	1.997
Ref. 9			——	——	0.008	1.128	0.158	2.065
Ref. 16[b]			——	——	0.034	1.144	0.146	2.083
Present[a]	1.05	Q_{12}	3.547	——	3.828	0.138	3.689	0.079
Ref. 7[b]			3.542	——	3.800	0.134	3.648	0.036
Ref. 9			3.880	——	3.955	0.255	3.781	−0.035
Ref. 16[b]			3.787	——	4.000	0.088	3.806	0.004
Present[a]	1.05	Q_{21}	——	——	−0.176	−0.200	−0.325	−0.250
Ref. 7[b]			——	——	−0.174	−0.197	−0.320	−0.244
Ref. 9			——	——	−0.200	−0.193	−0.342	−0.200
Ref. 16[b]			——	——	−0.185	−0.204	−0.333	−0.251
Present[a]	1.05	Q_{22}	−1.311	——	−0.581	0.754	−0.256	0.798
Ref. 7[b]			−1.293	——	−0.571	0.749	−0.247	0.790
Ref. 9			−1.339	——	−0.544	0.837	−0.162	0.797
Ref. 16[b]			−1.363	——	−0.590	0.790	−0.250	0.825

[a] See text for discretization details. [b] As reported in Refs. 8 and 9.

an expansion of the integrand is necessary to isolate the singularities. The following expression results after algebraic manipulation:

$$\left[\frac{\cos Kr}{r^3} + \frac{K \sin Kr}{r^2}\right] = \frac{1}{r^3} + \frac{1}{2!}\frac{K^2}{r} - \frac{3}{4!}K^4 r + \frac{5}{6!}K^6 r^3 \ \ldots \tag{7}$$

The first term on the right-hand side is the steady-state term, that is, the induced velocity at the wing plane due to a supersonic point doublet. For a constant density panel, its surface integral is equivalent to the induced velocity of a supersonic line vortex loop along the panel side. The second term corresponds to a source potential uniformly distributed over the panels with density K^2 and is also known from steady-state supersonic panel methods. In the present work, for numerical convenience, this term is integrated analytically along the y direction, and numerically along the streamwise x direction. For all other terms, actually only the next two ones in practice, the integration is completely numerical: each panel is divided into 100 points, and the Gauss–Legendre numerical quadrature method is used. From a numerical point of view, the use of complex variables allows for simpler integration subroutines because outside the Mach cones all terms in Eq. (7) become pure imaginary numbers. Therefore, if one only considers the real part of the quadrature process, there is no need to identify where Mach lines cross a given panel boundary. (This procedure automatically takes into account the right integration limits.)

Results and Discussion

Numerical calculations for a rectangular wing are described here. The largest configuration analyzed, corresponding to 480 panels, takes 10 min in a Pentium 100 MHz (this is evidently not a CPU time comparable to finite difference methods), where most of the time is spent setting up the influence coefficient matrix. This time is quite small, and it can get even smaller if the hyperbolic nature of the problem, due to the supersonic flow, is considered when assembling the matrix and solving the problem.

Figure 2 shows unsteady results regarding the two-dimensional portion of a wing oscillating in pitching about the leading axis. For unsteady calculations, the adequacy of the discretization is ascertained using steady-state values for the lift coefficient and pressure center. Here $M = 1.25$ and $k_r = 1$, such that $K = 2.22$. Comparison with two-dimensional calculations[15] in Fig. 2 reveals that a discretization of 20 elements along the chord is enough to obtain good agreement between complex potential results. However, since evaluation of the pressure coefficient demands numerical differentiation, one can see that the use of 20 panels still leads to some discrepancies. Comparison among results becomes better if the discretization is increased to 40 elements along the chord, which implies that the method is consistent even for high values of K.

Finally, generalized aerodynamic coefficients for a rectangular wing are obtained by integrating the pressure and the displacement modes, that is,

$$Q_{mn} = \iint_{\text{wing}} \Delta C_{pn} h_m \, \mathrm{d}x \, \mathrm{d}y \tag{8}$$

Converged results for M equal to 1.2 and 1.05 are presented in Table 1 (Refs. 7–9 and 16). Note that for all calculations leading to the results of Table 1, the real and imaginary parts of the pressure center were converged for the grids used, implying that the chordwise pressure distributions had reached their final form. However, the values of the generalized coefficients were clearly not converged, leading to the necessity of doing the linear extrapolation suggested by Rowe,[17] where the independent variable employed in the extrapolation process is the inverse of the number of panels along the chord. The $M = 1.2$ results were obtained using 40×8 and 45×9 grids, and it must be pointed out that both discretizations present the same panel aspect ratio. Although the overall agreement is very good between all methods studied, the present calculations are very close to those using the integrated-downwash model due to Stark.[7] One can also see from Table 1 that the agreement among results remains good for $M = 1.05$. Because in this case $1.5 < K < 3.1$, more refined discretizations along the chord are employed, that is, 45×6 and 60×8. Here the chordwise pressure distribution is very wavy, at least for $k_r = 0.3$.

Final Remarks

It has been shown that the present formulation gives excellent agreement both with analytical results (bidimensional region at the symmetry line) and numerical results (generalized aerodynamic coefficients) from other references. In the latter case, the authors consider that the extrapolation process to an "infinite" grid is necessary to guarantee converged values of the coefficients.

Another important point is that the generalized supersonic vortex-lattice method is an extension of the method in the case of subsonic regime. This is possible due to the use of a constant density doublet distribution over the wing (and wake, if necessary). For the aerodynamicist this is useful because this singularity is familiar and well known.

Acknowledgment

This research was supported by Empresa Brasileira de Aeronáutica S.A., CNPq—Conselho Nacional de Desenvolvimento Científico e Tecnológico (Grant 300.682/93-0).

References

[1]Yates, E. C., "Unsteady Subsonic and Supersonic Flows—Historical Review; State of the Art," *Computational Methods in Potential Aerodynamics*, Springer–Verlag, Berlin, 1985, pp. 96–137.

[2]Cunningham, A. M., Jr., "Oscillatory Supersonic Kernel Function for Interfering Surfaces," *Journal of Aircraft*, Vol. 11, No. 11, 1974, pp. 664–670.

[3]Lottati, I., and Nissim, E., "Nonplanar, Supersonic, Three-Dimensional, Oscillatory, Piecewise Continuous-Kernel Function Method," *Journal of Aircraft*, Vol. 24, No. 1, 1987, pp. 45–54.

[4]Ueda, T., and Dowell, E. H., "Doublet-Point Methods for Supersonic Unsteady Lifting Surfaces," *AIAA Journal*, Vol. 22, No. 2, 1984, pp. 179–186.

[5]Appa, K., "Constant Pressure Panel Method for Supersonic Unsteady Airload Analysis," *Journal of Aircraft*, Vol. 24, No. 10, 1987, pp. 696–702.

[6]Pines, S., Dugundji, J., and Neuringer, J., "Aerodynamic Flutter Derivatives for a Flexible Wing with Supersonic and Subsonic Edges," *Journal of the Aeronautical Sciences*, Vol. 22, No. 10, 1955, pp. 693–700.

[7]Stark, V. J. E., "Calculation of Aerodynamic Forces on Two Oscillating Finite Wings at Low Supersonic Mach Number," SAAB, TN 53, Linköping, Sweden, Feb. 1964.

[8]Appa, K., and Jones, W. P., "Integrated Potential Formulation of Unsteady Supersonic Aerodynamics for Interacting Wings," *Journal of Aircraft*, Vol. 13, No. 9, 1976, pp. 695–703.

[9]Jones, W. P., and Appa, K., "Unsteady Supersonic Aerodynamic Theory by the Method of Potential Gradient," *AIAA Journal*, Vol. 15, No. 1, 1977, pp. 59–65.

[10]Chen, P.-C., and Liu, D. D., "A Harmonic Gradient Method for Unsteady Supersonic Flow Calculations," *Journal of Aircraft*, Vol. 22, No. 3, 1985, pp. 371–379.

[11]Miles, J. W., *The Potential Theory of Unsteady Supersonic Flow*, Cambridge Univ. Press, Cambridge, England, UK, 1959, p. 36.

[12]Epton, M. A., "Integration-by-Parts Formulas for Boundary-Element Methods," *AIAA Journal*, Vol. 30, No. 2, 1992, pp. 496–504.

[13]Miranda, L. R., Elliot, R. D., and Baker, W. M., "A Generalized Vortex Lattice Method for Subsonic and Supersonic Flow Applications," NASA CR 2865, Dec. 1977.

[14]Soviero, P. A. O., and Bortolus, M. V., "Generalized Vortex Lattice Method for Oscillating Lifting Surfaces in Subsonic Flow," *AIAA Journal*, Vol. 30, No. 11, 1992, pp. 2723–2729.

[15]Soviero, P. A. O., and Ribeiro, R. S., "Panel Method Formulation for Oscillating Airfoils in Supersonic Flow," *AIAA Journal*, Vol. 33, No. 9, 1995, pp. 1659–1666.

[16]Fenain, M., and Guiraud-Vallée, D., "Numerical Calculation of Wings in Steady or Unsteady Supersonic Flow, 2nd Part: Unsteady Flow," *Recherche Aerospatiale*, No. 116, Jan.–Feb. 1967, pp. 23–33.

[17]Rowe, W. S., "Unsteady Subsonic and Supersonic Flows—Historical Review; State of the Art," *Computational Methods in Potential Aerodynamics*, Springer–Verlag, Berlin, 1985, pp. 197–240.

A. Plotkin
Associate Editor

Effect of Yaw on Pressure Oscillation Frequency Within Rectangular Cavity at Mach 2

Peter J. Disimile* and Paul D. Orkwis†
University of Cincinnati,
Cincinnati, Ohio 45221-00070

Nomenclature

D	= cavity depth, cm
f_D, f_L, f_W	= fundamental acoustic modes based on cavity depth, length, and width, Hz
$f_{e,m}$	= Rossiter's edgetone frequency for mode m equal to 1, 2, 3, ..., Hz
f_v	= vortex shedding frequency, Hz
L	= cavity dimension along the minor axis, cm
M_∞	= freestream Mach number
Re_θ	= Reynolds number based on the boundary layer momentum thickness
Sr_θ	= Strouhal number based on momentum thickness, $f_v\theta/U_\infty$
U_∞	= freestream velocity, m/s
W	= cavity dimension along the major axis, cm
θ	= momentum thickness of the approaching boundary layer, mm
ψ	= yaw, the angle between U_∞ and cavity minor axis L, deg

Introduction

THE presence of a cavity in a surface bounding a fluid flow can cause large pressure, velocity, and density fluctuations in its vicinity as well as strong propagating acoustic waves. In addition, the drag on the surface can be altered, sensitive instrumentation can be damaged, and structural failure due to resonance can occur. Such flows are of interest in many different areas of engineering. Landing-gear wells, surface-mounted optical instrumentation, and bomb bays on aircraft are common examples of cavities in which reduction of pressure fluctuations, vibration, noise generation, and sonic fatigue are of prime concern.

Supersonic cavity flowfields contain a mixture of unsteady flow regimes that may include unstable shear layers that shed vortices in coherent patterns, unsteady weak shock or pressure waves, and resident vortices oriented in the transverse direction. This interaction is the result of an extremely complicated flow pattern that appears to depend on the shape of the cavity, freestream Mach number, Reynolds number, and the characteristics of the approaching boundary layer. Many prior investigations[1–4] have been conducted to gain insight into the underlying physical behavior of cavity flows. These studies, including that of Rossiter,[5] have made it possible to predict some features of the observed phenomena. Unfortunately,

Received Aug. 30, 1996; revision received March 4, 1997; accepted for publication April 7, 1997.

*Associate Professor, Department of Aerospace Engineering. Member AIAA.

†Assistant Professor, Department of Aerospace Engineering. Member AIAA.